A preliminary approach to the ALFRED reactor control strategy

Roberto Ponciroli, Antonio Cammi, Stefano Lorenzi, Lelio Luzzi*

Politecnico di Milano, Department of Energy, CeSNEF (Enrico Fermi Center for Nuclear Studies), via Ponzio 34/3, 20133 Milano, Italy

Article history:
Received 24 May 2013
Received in revised form
17 December 2013
Accepted 27 January 2014

1. Introduction

The main purpose of the control system in Nuclear Power Plants (NPPs) is adjusting the reactor power in accordance with the system demands in a consistent and constrained way. The control system development represents a crucial issue in the design process since the nuclear reactor is a part of an integrated plant including ultimately the load in the form of electrical grid. "Consistent and constrained way" means that the control system has to ensure the optimum working conditions for the system, avoiding the need for the protection system to shutdown the plant during operational transients (Lewins, 1978; Bernard, 1999).

A particular attention to these aspects should be paid whether an innovative NPP is considered because of the safety concerns which may be different from the ones of water-cooled reactors. In particular, for the Lead-cooled Fast Reactor (LFR), selected by the Generation IV International Forum as one of the candidates for the next generation of nuclear power plants (GIF, 2002), the need of developing an effective control strategy has been recognized. Actually, the control scheme requirements due to the technological issues brought by the use of lead as coolant (Tucek et al., 2006) have not been investigated yet. In this perspective, the main focus of this paper consists in developing a preliminary attempt to the control strategy definition of LFRs, adopting as a reference plant the Advanced Lead Fast Reactor European Demonstrator (ALFRED) (Alemberti et al., 2013), developed within the European FP7 LEADER Project (http://www.leader-fp7.eu, 2012).

The design of a NPP control system is a multi-step process whose final result is the development of dedicated controllers. First of all, it is necessary to prove the intrinsic system stability and to assess the control system robustness at different operational conditions. In particular, it is important that no problems arise in certain crucial transients, e.g., during the start-up sequence or following any change of load in full power conditions. Secondly, the

* Corresponding author.
E-mail address: lelio.luzzi@polimi.it (L. Luzzi).

reactor dynamics should be deeply investigated since these aspects are fundamental for the study of the overall plant performance. Moreover, this analysis allows investigating the interactions among input and output variables providing fundamental insights on stability and useful guidelines for the conception of an appropriate control system.

In order to perform such analyses, two flexible, straightforward, and fast-running simulators have been sought expressly meant for this early phase of the ALFRED design, during which all the system specifications are still considered as open design parameters and thus may be subject to frequent modifications. Such tools have been conceived for: (i) evaluating the robustness and stability of the dynamic system itself on its entire power range thanks to the possibility of linearizing the constitutive equations around different working conditions; (ii) predicting the reactor response to typical transient initiators and thus obtaining more detailed information about its dynamic behaviour; and (iii) helping the control system implementation for both its realization and its validation.

As far as the first item (i) is concerned, an analytical zero-dimensional model allowing for all the main reactivity feedbacks has been developed (Bortot et al., 2013). The resulting nonlinear model has been linearized and then implemented in MATLAB® (MATLAB® and SIMULINK® software, 2005) so as to verify the reactor stability through the calculation of the system eigenvalues. As a major result of this study, considering both a stand-alone core and a primary loop configuration, the system has been tested to be inherently stable on the entire power range. Moreover, the governing dynamics of the system has been identified, underlining the fundamental impact of the coolant density reactivity coefficient on the system stability and control strategy.

Concerning items (ii) and (iii), a one-dimensional, nonlinear *object-oriented* simulator has been developed (Ponciroli et al., 2014) by employing the reliable, tested, and well-documented Modelica language (Fritzson, 2004). Such tool has been specifically addressed to transient analyses as its detailed geometry description allows getting more accurate simulation results. As far as the core is concerned, point reactor kinetics and heat transfer models have been implemented coherently with the ALFRED specifications by incorporating geometry, material properties and correlations, reactivity feedback coefficients, and kinetic parameters (Grasso et al., 2013). An effort has been spent to build a specific model for the Steam Generators (SGs) due to their non-conventional bayonet-tube design, in order to reproduce their characteristic configuration (Alemberti et al., 2013), whereas specific models have been selected to describe the fluid flows (i.e., two-phases for water and single phase for lead). Several design-basis transient scenarios have been simulated to characterize the system dynamic behaviour and to evaluate the most effective inputs and their influence on the output variables to be properly controlled.

As far as LFRs are concerned, the control approach adopted in acknowledged reactor concepts, such as Light Water Reactors (LWRs) and Sodium-cooled Fast Reactors (SFRs), cannot be immediately applied due to the different features related to the use of lead as coolant and resulting in several constraints on control and controlled variables. The most challenging issue regards the lead temperature in the cold pool, which has to be kept in a narrow range, in addition to the lower limit fixed by the coolant solidification (327 °C). In particular, the vessel temperature should not exceed 420 °C (thermal creep threshold), whereas the minimum temperature is fixed at 380 °C due to the embrittlement of the structural materials in aggressive environment enhanced by the fast neutron irradiation. Consequently, the currently adopted approach cannot be immediately applied, but it is necessary to define a proper control strategy based on the system dynamics and taking into account the technological constraints of the plant.

In this perspective, a first approach to the control strategy of an innovative LFR concept has been developed. Given that for the considered system neither prior experience nor operational data are available, it has been considered necessary to adopt a quantitative well proven investigation tool. Therefore, the indications provided by the simulation of the system governing dynamics have been supported by a dedicated quantitative technique such as the *Relative Gain Array* (RGA) method (Bristol, 1966). This tool allows developing the most efficient control strategy starting from the constitutive equations that describe the physical system taken into account. In particular, this method has been widely used in several industrial fields including chemical processes and power production (Papadourakis et al., 1987), and recently adopted in nuclear applications as well (Guerrieri et al., 2014).

This work constitutes a preliminary stage of the control system design, adopting an existing and reliable technique (such as the RGA) for the pairing selection of a Generation IV LFR, whose control strategy has never been deeply studied (no dedicated papers have been found in the literature). In this way, through the RGA approach, it has been possible to evaluate the impact and the effectiveness of two different control strategies, based on different control variables, and to compare the performance of the proposed control solutions.

The paper is organized as follows. In Section 2, a brief introduction to the ALFRED reactor is provided. In Section 3, the main features of the object-oriented model of the overall plant, which has been employed both to develop and to assess the proposed control strategies, are summarised. In Section 4, the RGA technique has been adopted to select the most effective pairings between the control and the controlled variables. In Sections 5 and 6, the regulators implemented in the adopted control schemes are described and the importance of the lead mass flow rate in the primary circuit as a system input is investigated. Finally, in Section 7, two controlled operational transients have been simulated and the outcomes are discussed.

2. Reference reactor description

ALFRED is a small-size (300 MW_{th}) pool-type LFR and its primary system current configuration is depicted in Fig. 1. All the primary components (e.g., core, primary pumps and SGs) are contained in the main reactor vessel, being located in a large pool within the reactor tank. The coolant flow coming from the cold pool enters the core and, once passed through the latter, is collected in a volume (hot collector) to be distributed to eight parallel pipes and delivered to as many SGs. After leaving the SGs the coolant enters the cold pool through the cold leg and returns to the core.

The ALFRED core is composed by wrapped hexagonal Fuel Assemblies (FAs) with pins arranged on a triangular lattice. The 171 FAs are subdivided into two radial zones with different plutonium fractions guaranteeing an effective power flattening, and surrounded by two rows of dummy elements serving as a reflector. Two different and independent control rod systems have been foreseen, namely, Control Rods (CRs) and Safety Rods (SRs), which are assigned regulation/compensation and scram functions assuring the required reliability for cycle reactivity swing control and safe shut-down (Grasso et al., 2013).

Each of the eight SGs incorporated in ALFRED (Fig. 2) consists of bundles of bayonet vertical tubes with external safety tube and internal insulating layer (delimited by a slave tube), which is aimed at ensuring the production of superheated dry steam since, without a proper insulation, the high temperature difference between the rising steam and the descending feedwater promotes steam condensation in the upper part of the SG. The gap between the outermost and the outer bayonet tube is filled with pressurized

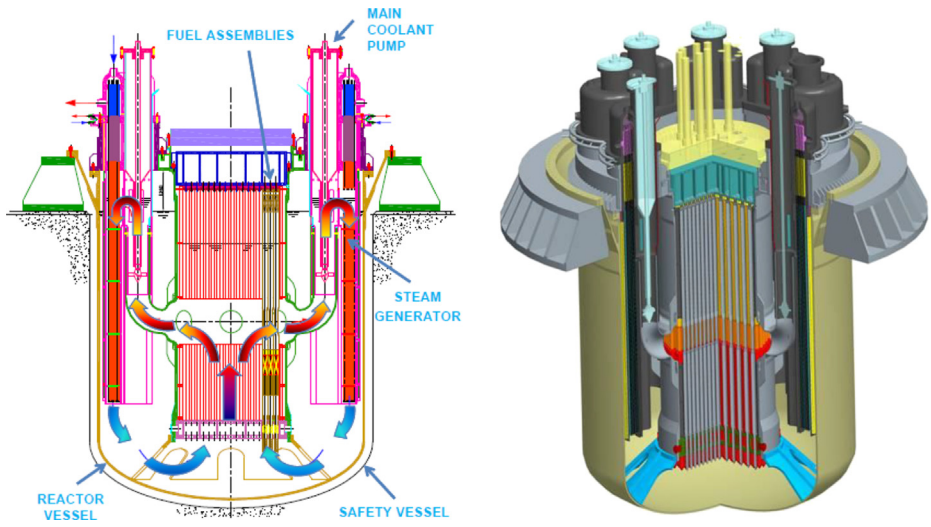

Fig. 1. ALFRED primary system and core layouts (Alemberti et al., 2013).

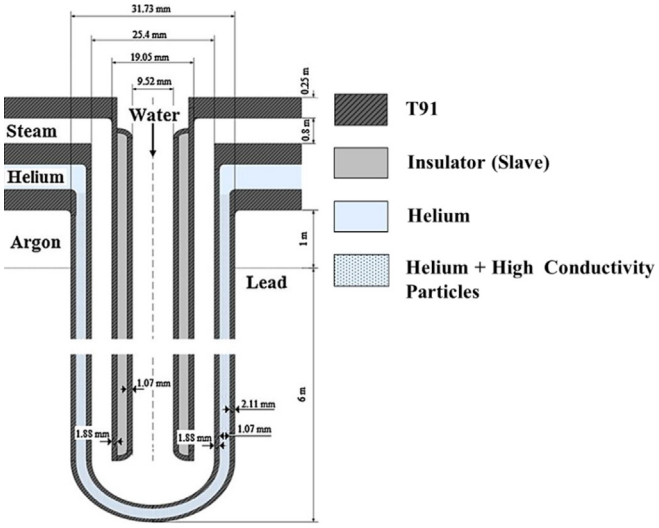

Fig. 2. ALFRED bayonet tube configuration (Alemberti et al., 2013; Damiani et al., 2013).

helium and high thermal conductivity particles to enhance the heat exchange capability and provide mechanical decoupling between the components. The feedwater from the headers flows in the slave tube and, after reversing the motion at the bottom, rises along the annulus between inner and outer tubes. On the primary side, lead flows downwards axially along the outermost tube. In Table 1, the major parameters employed as input data to implement the core and SG models are resumed.

3. Alfred reactor object-oriented model description

In this work, the proposed control strategies have been developed and assessed by means of an object-oriented model of the ALFRED reactor. The simulator of the overall plant has been implemented in the Dymola environment (DYNASIM software, 2006; Elmqvist et al., 1993), which also gives the possibility of linearizing the system of equations in the neighbourhood of the equilibrium condition (i.e., nominal power, 300 MW_{th}). In Fig. 3, the layout of the plant model is represented to point out the main

Table 1
ALFRED system parameters.

Parameter	Value	Units
Thermal power	300	MW_{th}
Coolant mass flow rate	25,984	kg s^{-1}
Coolant SG outlet temperature	400	°C
Coolant core outlet temperature	480	°C
Pool temperature during cold shutdown	380	°C
Feedwater mass flow rate	192	kg s^{-1}
Water inlet temperature	335	°C
Steam outlet temperature	450	°C
SG pressure	180	bar

components of the plant and the respective input variables (blue triangles) and output variables (white triangles). The system simulator has been realized by connecting several dedicated models (see Ponciroli et al. (2014) for details):

- *Core model*: it is composed by three subsystems. The model *Kinetics* describes the dynamics of the neutron generation processes in the core implementing a point kinetics approach, with one neutron energy group and six delayed precursor groups. The model *FuelRods* is adopted to represent the thermal behaviour of the fuel pins, which are discretized in five radial regions (i.e., the cladding, the gap and three concentric zones within the pellet). The model *LeadTube* represents the coolant flowing through the core channels adopting one-dimensional mass, momentum and energy conservation equations.
- *SG model*: as far as the water side is concerned, a two-phases homogeneous model (i.e., same velocity for the liquid and vapour phases), has been adopted. On the lead side, the core component *LeadTube* is reused, describing the behaviour of a single-phase fluid.
- *Primary circuit model*: the dynamics effects of the cold pool have been represented by employing a free-surface cylindrical tank component on which mass and energy balances are taken into account, assuming that no heat transfer occurs except through the inlet and outlet flows. In order to consider the time delay due to the transport phenomena between the core and the SG, two dedicated models have been implemented. As far as the integrated primary pump is concerned, an ideal mass flow rate regulator has been employed.

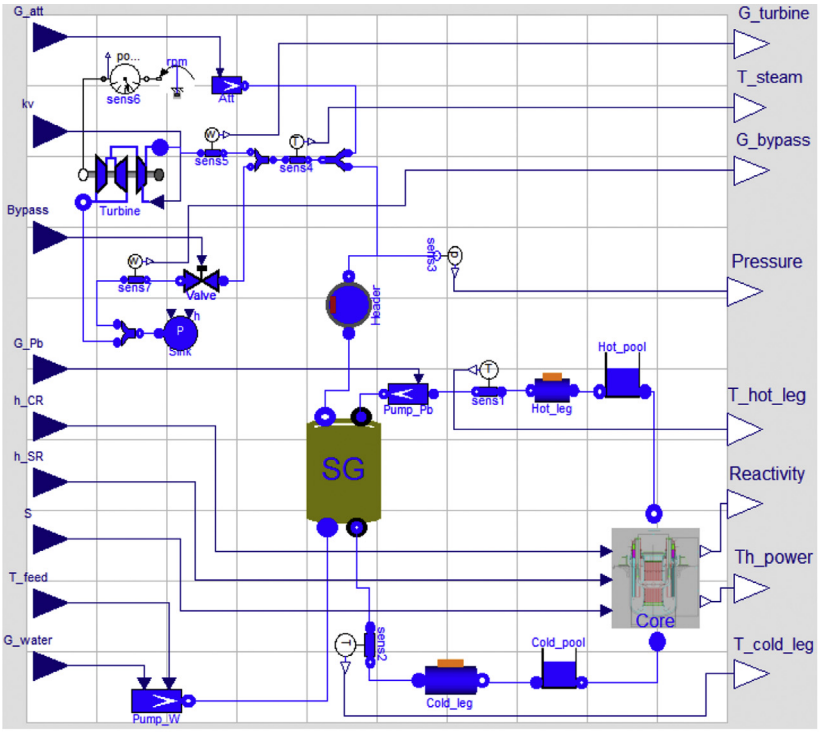

Component	Description
Core	Reactor core
Cold_pool	Pool collecting the lead coming from the SG outlet
Cold_leg	Collector between the SG outlet and the core inlet
Hot_pool	Pool collecting the lead coming from the core outlet
Hot_leg	Collector between the core outlet and the SG inlet
sens	Temperature and pressure sensor placed in the plant
Pump_Pb	Lead axial pump
SG	Steam generator
Header	Volume collecting the produced steam
Pump_W	Water pump
Turbine	Steam turbine unit
Sink	Condenser
Att	Attemperator allowing to regulate the steam temperature

Input variable	Definition
G_att	Attemperator mass flow rate
kv	Turbine admission valve coefficient
Bypass	Bypass valve coefficient
G_Pb	Primary circuit lead mass flow rate
h_CR	Control rod height
h_SR	Safety rod height
S	Neutron source
T_feed	Feedwater inlet temperature
G_water	Feedwater mass flow rate

Output variable	Definition
G_turbine	Turbine admitted mass flow rate
T_steam	Turbine inlet steam temperature
G_bypass	Bypass discharged mass flow rate
Pressure	SG pressure
T_hot_leg	Temperature of lead flowing out of the core
Reactivity	System reactivity
Th_power	Thermal power produced within the core
T_cold_leg	Temperature of lead flowing into the core

Fig. 3. Graphical interface of the object-oriented model of the overall ALFRED plant (Ponciroli et al., 2014).

- *Secondary circuit model*: the model selected for the turbine describes a simplified steam turbine unit, in which a fraction of the available enthalpy drop is assumed to be converted by the High Pressure (HP) stage, whereas the remaining part to be converted by the Low Pressure (LP) one, with different time constants. The steam mass flow rate is considered proportional to the inlet pressure and governed by operating on the turbine valve admission (k_v), not by throttling. Downstream of the steam temperature sensor, the steam mass flow rate can follow two ways. The former is a pipe that leads to the turbine, whereas the latter constitutes a bypass, which leads directly to the condenser. Thanks to the adoption of a bypass, it is possible to employ this model to simulate the start-up phase. Indeed, when the thermal power from the primary circuit is not sufficient to ensure the steam nominal conditions, the flow is directly disposed to the condenser to avoid jeopardizing the integrity of the turbine.

4. Pairing selection among control and controlled variables

In the definition of a suitable control strategy, once the system governing dynamics has been identified, the next step to be taken into account is the choice of the pairings between input and output variables. The aim of this stage is to evaluate the influence performed by the control variables (the system inputs, u_i) on the candidate controlled variables (the system outputs, y_i) in order to select the most effective couplings. A first option for the LFRs would have been the adoption of the well-proven control strategies employed in LWRs or SFRs. Nevertheless, despite these approaches rely on the wide experience gained in the past, it has not been possible to rearrange these concepts because of the new technological issues and safety concerns which characterize the LFRs. For these reasons, the RGA quantitative approach has been adopted to perform the *pairing selection*, i.e., the identification of the most effective input to regulate a specific output, according to the level of interaction (Bristol, 1966).

Generally, most of the physical systems may be modelled as *Multiple Inputs* and *Multiple Outputs* (MIMO) systems. The different input/output variables present structural connections that strictly limit the direct application of the control techniques developed for *Single Input Single Output* (SISO) systems (Skogestad and Postlethwaite, 2005). A possible solution is represented by the centralized scheme shown in Fig. 4a, in which a dedicated block (indicated with $\Delta(s)$) allows treating the MIMO system as if it were constituted by several uncoupled SISO systems, balancing the undesired cross influences between inputs and outputs. Nevertheless, such an option cannot be adopted if the system presents non-minimum phase behaviour and/or pure time delays as in the case of ALFRED reactor (Bortot et al., 2013). For this kind of systems, a

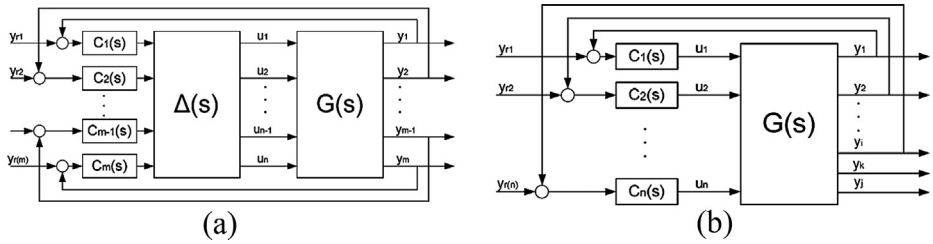

Fig. 4. Representation of a centralized control scheme (a), and of a decentralized control scheme (b). In particular, the physical process to be controlled ($G(s)$), the several implemented controllers ($C_i(s)$), the system output variables (y_i), the corresponding set-points (y_{ri}), and the system input variables (u_i) are shown.

specific decentralized control approach (Fig. 4b) has to be adopted, hence the undesired couplings between input and output cannot be compensated. Even if the performance of a decentralized scheme is poorer than the one of a centralized scheme, this configuration allows overcoming many limitations. In particular, the operation and maintenance of controllers are favoured by the simplicity of their implementation, and the resulting system is robust with respect to malfunctioning of the single control loops.

In a decentralized control scheme, the first step is constituted by the selection of the most effective pairings between control and controlled variables. Accordingly, the input showing the most relevant interaction with a certain output, and at the same time not significantly affecting the behaviour of other variables of interest, represents the ideal candidate to achieve a feedback control loop. Interactions among variables constitute a physical feature of the system, and the best hints for the coupling can be derived by analysing the free dynamics response of the plant. These indications can be supported by some dedicated techniques, such as the RGA method. This procedure is a heuristic method that allows to determine the most efficient input to control each variable of interest, providing useful suggestions on how the model-based decentralized control system should be structured.

The effectiveness of a feedback control loop can be assessed by characterizing the MIMO system behaviour both in *open loop* and *closed loop* conditions. As far as the open loop gain is concerned, considering the system at equilibrium condition for fixed constant values of control variables, a step variation of amplitude δu_i on a certain input u_i is performed, causing a variation of the quantity δy_{jOL} of each output variable y_j (Fig. 5a). The open loop gain is defined as

$$g_{ji} = G_{ji}(0) = \frac{\delta y_{jOL}}{\delta u_i} \tag{1}$$

where $G_{ji}(0)$ is regarded as the gain of the transfer function between u_i and y_j. Instead, for the closed loop gain, it is assumed that, against the same variation of δu_i, an action is performed on all the other input variables in order to keep all the other outputs fixed, except for y_j, thanks to the action carried out by the other inputs (Fig. 5b). If the variation of y_j in closed loop configuration is indicated with δy_{jCL}, the closed loop gain between u_i and y_j can be defined as

$$h_{ji} = \frac{\delta y_{jCL}}{\delta u_i} \tag{2}$$

If the static gain for the open loop (g_{ji}) and for the closed loop (h_{ji}) are evaluated for all the input–output pairs, the RGA matrix Λ can be obtained. This matrix can be regarded as a quantitative measure of the input–output interaction at zero frequency for asymptotically stable processes. In particular, the elements λ_{ji} of this matrix, namely the relative gain of the pair (u_i, y_j), are defined as:

$$\lambda_{ji} = \frac{g_{ji}}{h_{ji}} \tag{3}$$

In a control system development perspective, when the value of a λ_{ji} element approaches unity, there is a fair interaction that can be exploited, whereas if the value of a λ_{ji} element approaches zero the involved variables can be regarded as uncoupled. If the matrix element λ_{ji} is negative, it means that the control action may produce effects opposite to the desired ones on the controlled variable, depending on whether feedback control loops involve other output variables or not (Skogestad and Postlethwaite, 2005).

In common applications, the RGA matrix cannot always be applied since the physical system must have the same number of inputs and outputs. Most of the systems present a number of outputs that is higher than the number of inputs, and thus it is necessary to redefine a formal procedure for the choice of input–output pairs. Such a procedure is offered by the *Non-square Relative Gain array* (NRG) (Chang and Yu, 1990). In this case, the pairing process is performed in two phases: (i) the less relevant outputs are disregarded in order to obtain a square input–output matrix; and (ii) the choice of the input–output pairs. The first stage is performed by computing the sum of the elements on each row of the NRG matrix, which produces the Row Sum (RS) vector. The outputs associated to the largest figures of the RS vector are the most influenced ones by the inputs variation and thus the most relevant

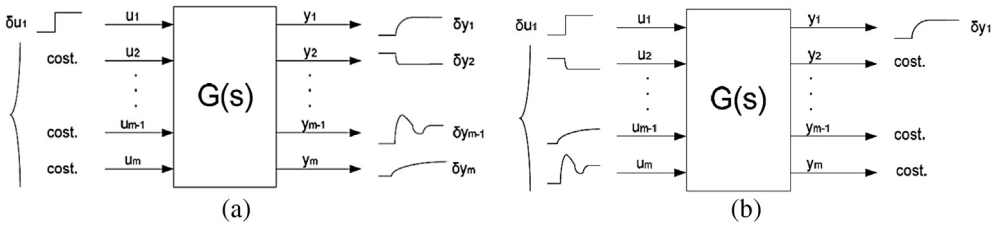

Fig. 5. Representation of an open loop response (a), and of a closed loop response (b). In particular, the physical process to be controlled ($G(s)$), the system output variables (y_j), the corresponding variation (δy_j), the system input variables (u_i), and the corresponding variation (δu_i) are shown.

in a control perspective. At this point, the choice of the pairs can be made either through the RGA matrix of the reduced system or through the NRG matrix after having removed the rows concerning the outputs considered useless for the control, adopting the same selection criterion used in the RGA approach.

5. Alfred control strategy definition

In a NPP, the main system output to be controlled is the thermal power produced within the core. As far as the conventional part of the plant is concerned, the other controlled variables are the SG pressure and the steam temperature at the turbine inlet, which should be kept as close as possible to their respective nominal values. The main advantages of running the SG at constant pressure (i.e., the current procedure in the Rankine cycle-based power plants) is the possibility of quickly varying the power produced so as to be adapted to the load required by the grid, and the possibility to avoid thermo-mechanical stresses in the SG when the load varies. On the other hand, this kind of control determines additional costs for the regulators, and the pumps usage remains unnecessarily high at reduced loads conditions.

As far as the ALFRED primary loop is concerned, the most constrained output that must be efficiently controlled is the SG outlet lead temperature, called also *cold leg temperature*. The nominal value of 400 °C represents the optimum working condition for this variable. Temperatures below this limit would lead to a degradation of structural steels due to the embrittlement enhanced by neutron irradiation. On the other hand, if the inlet lead temperature rises beyond this value, the reactor vessel may overcome the design limit concerning thermal creep.

As common in nuclear plants experiences, the examined system has turned out to be *underactuated*, i.e., the manageable inputs (control variables) are fewer than the variables to be controlled. Among the possible control variables, the coolant mass flow rate in the primary loop represents a key issue in the definition of the control strategy for the ALFRED reactor. One of the major efforts in the development of LFR concept is the design of pumps which operate in the highly aggressive lead environment. In the reactor layout, the coolant is currently envisaged to be driven by an axial pump requiring a constant number of revolutions per minute. Moreover, working at nominal mass flow rate also for power levels lower than the nominal one brings benefits as far as structural materials are concerned since they would operate at reduced temperatures with consequent positive effects on corrosion. Despite these considerations, it may be worthwhile considering the possibility to adopt the lead mass flow rate in the primary loop as a control variable to ensure a more flexible control action. Therefore, two control schemes have been studied in order to evaluate the consequences on the control system definition of considering it either as a system input, or as a parameter which remains fixed at different working conditions.

In order to develop a control system for the ALFRED reactor, the object-oriented simulator of the entire plant described in Section 3 has been first employed with the main purpose of studying the system free dynamics to understand the basic relationships between input and output variables. After having linearized the system around nominal condition, the NRG method has been applied. Based on both the outcomes of the ALFRED free dynamics investigations and the results of the NRG analysis, a decentralized control scheme has been chosen because of the presence of non-minimum phases and pure time delays mainly due to the reactor pool-type configuration. Two control strategies have been proposed and discussed depending on whether the lead mass flow rate is considered or not as a control variable. Finally, both configurations have been implemented and the performance of each proposed control strategy has been evaluated, as described in the following sub-Sections 5.2 and 5.3.

5.1. Plant model linearization

As it has been stated in Section 3, the dedicated object-oriented model has been linearized in the neighbourhood of the nominal power conditions by means of a useful feature of the Dymola simulation environment. As a result of this operation, the resulting model has been expressed by adopting the matrix-based form of the Linear Time-Invariant (LTI) systems

$$\begin{cases} \delta\dot{x}(t) = A\delta x(t) + B\delta u(t) \\ \delta y(t) = C\delta x(t) + D\delta u(t) \end{cases} \tag{4}$$

A 194th order system has been obtained and it is necessary to reduce the system to a more suitable and manageable size. There are several procedures that can be implemented to get a satisfactory order reduction and there are several examples in literature (Moore, 1981; Van Dooren, 2000). Hereafter, the methodology adopted by MATLAB® will be referred, which provides precompiled functions to reduce LTI models. It consists in an appropriate coordinate transformation, which allows obtaining a balanced and equivalent representation, in terms of system state variables, so that observability and reachability Gramians result to be equal and diagonal (Moore, 1981). The balanced model that is obtained is then defined by

$$\begin{cases} \delta\dot{\tilde{x}}(t) = \tilde{A}\delta\tilde{x}(t) + \tilde{B}\delta\tilde{u}(t) \\ \delta\tilde{y}(t) = \tilde{C}\delta\tilde{x}(t) + \tilde{D}\delta\tilde{u}(t) \end{cases} \tag{5}$$

where

$$\begin{aligned} \tilde{A} &= T_L^{-1} A T_L \\ \tilde{B} &= T_L^{-1} B \\ \tilde{C} &= C T_L \\ \tilde{D} &= D \end{aligned} \tag{6}$$

The matrix that realizes the change of coordinates is indicated with T_L and it can be obtained according to the procedure indicated by Laub et al. (1987). At this point, the order of the balanced system has been reduced by removing the undesired states, obtaining a 43rd order system. After deriving the corresponding matrices of this new system, it is necessary to validate these approximations showing that the linearized reduced order model allows us to effectively reproduce the system evolution during operational transients. In Fig. 6, a comparison between the non-linear model and the linear and reduced model is shown, confirming the accuracy of the adopted approximation.

5.2. Five-input control strategy

As shown in Fig. 7, the lead mass flow rate (*G_Pb*) is operated as a system input in the 5-input control strategy. The outcomes achieved by means of the NRG method, shown in Table 2, suggest to use this control variable to maintain the lead temperature in the cold leg (*T_cold_leg*) close to its nominal value. In addition, the values representing the interactions between lead mass flow rate and other outputs are sufficiently low so as to allow the closure of a feedback control loop without problematic interactions with other output variables. As far as the remaining control loops are concerned, it appears clear that the steam temperature (*T_steam*) and mass flow rate (*G_turbine*) can be governed by the feedwater temperature (*T_feed*) and mass flow rate (*G_water*), respectively. On

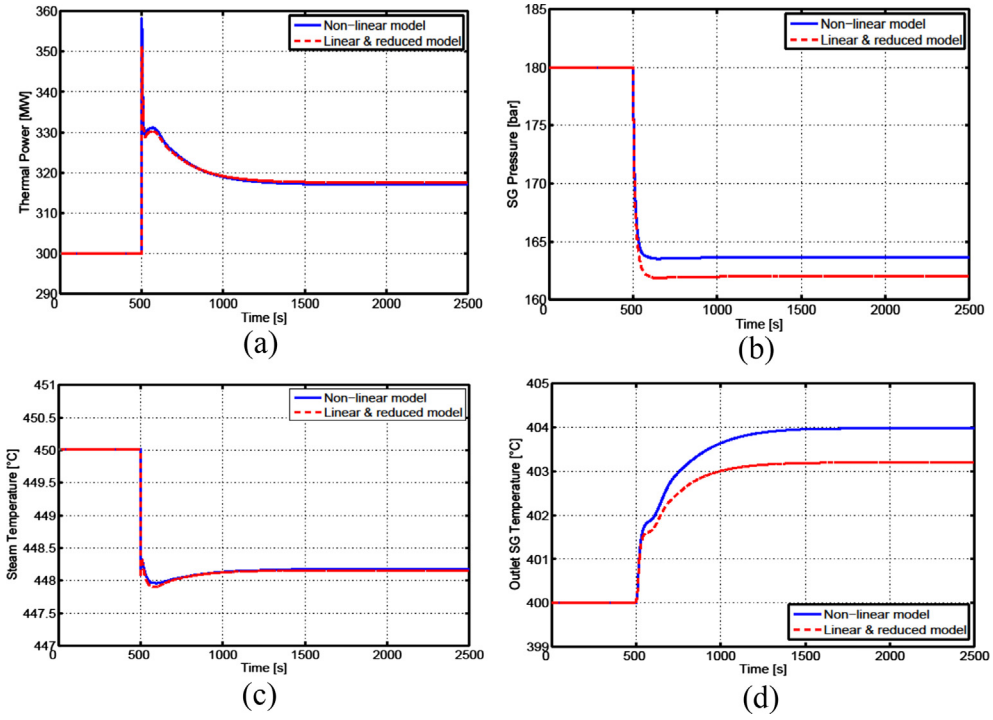

Fig. 6. Comparison between linearized model and non-linear model responses: (a) power transient following a step input given on the control rods position (−3 mm), (b) pressure transient following a step input given on the turbine admission (+0.1), (c) steam temperature transient following a step input given on the attemperator mass flow rate (+1 kg/s), (d) temperature in the cold leg transient following a step input given on the water mass flow rate (−5%).

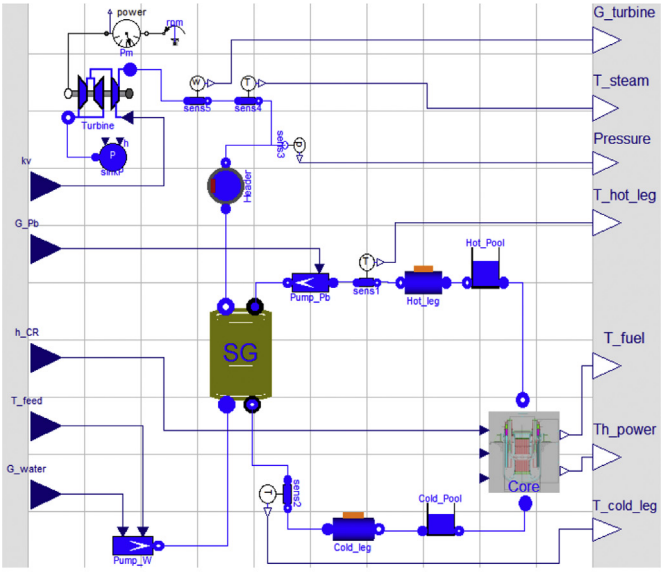

Input variables	Definition
kv	Turbine admission valve coefficient
G_Pb	Lead mass flow rate
h_CR	CR height
T_feed	Feedwater inlet temperature
G_water	Feedwater mass flow rate
Output variables	**Definition**
G_turbine	Turbine admitted mass flow rate
T_steam	Turbine inlet steam temperature
Pressure	SG pressure
T_hot_leg	Temperature of lead flowing out of the core
T_fuel	Temperature of the fuel pin
Th_power	Thermal power produced within the core
T_cold_leg	Temperature of lead flowing out of the SG

Fig. 7. Object-oriented model of the ALFRED reactor by adopting the 5-input control strategy.

Table 2
Pairing selection performed by means of the NRG method (5-input control strategy). The rows in grey represent the outputs that have been discarded for control purposes, whereas red values represent the elements that correspond to the chosen input/output pairs.

OUTPUTS	INPUTS				
	T_feed	*G_water*	*h_CR*	*G_Pb*	*kv*
T_steam	**0.4169**	0.0082	0.1729	0.0274	−0.0006
T_fuel	0.0478	0.0003	0.2683	−0.0008	−0.0002
Pressure	0.0000	−0.0021	−0.0000	−0.0000	**0.9989**
G_turbine	−0.0000	**0.9986**	−0.0000	−0.0000	−0.0000
T_cold_leg	0.1597	−0.0019	0.0741	**0.5911**	0.0007
Th_power	0.2757	−0.0007	**0.4267**	−0.0018	0.0004
T_hot_leg	0.1000	−0.0024	0.0581	0.3841	0.0009

the other hand, the core power (*Th_Power*) and the SG pressure (*Pressure*) can be regulated by adjusting the CR position (*h_CR*) and the turbine admission valve opening (*kv*), respectively. Finally, two outputs out of seven have been necessarily excluded in order to control the remaining five with the available five inputs. In particular, the fuel (*T_fuel*) and the hot leg (*T_hot_leg*) temperatures have been left out since they are of secondary importance compared to the other output variables in the perspective of controlling the power plant. Moreover, the poor value of the feasible pairings induces to eliminate them since their control would not be very effective in any case.

5.3. Four-input control strategy

In the 4-input control strategy, the lead mass flow rate (*G_Pb*) is kept fixed at its nominal value, hence it does not constitute an input in the object-oriented model shown in Fig. 8. The lead temperature in the cold leg (*T_cold_leg*) must be governed by adopting another input, and the NRG outcomes suggest to use the feedwater temperature (*T_feed*), as shown in Table 3. This coupling, despite being the only way to regulate the SG outlet lead temperature, determines a series of issues which complicate the control scheme design making the system less flexible. First of all, when the lead mass flow rate is a system input (5-input control scheme, Table 2), the feedwater temperature is the second choice, indicating that the pairing (*T_feed*, *T_cold_leg*) is less efficient. Moreover, there are technological constraints strictly limiting the feedwater temperature range. In particular, the feedwater temperature at the SG inlet cannot exceed 355 °C (i.e., water saturation temperature at the SG nominal pressure) because this eventuality would produce severe damages to the pumps. In addition to this upper limit, there is a lower constraint given by the temperature of lead melting as well. In order to avoid local solidification, the feedwater temperature must always be kept higher than 327 °C. These boundaries determine strict restrictions on the use of this input, which can vary between −8 °C and +20 °C with respect to its nominal conditions.

As far as the remaining control loops are concerned, the core power can be controlled by regulating the position of CRs (*h_CR*), and the pressure within the SG (*Pressure*) can be controlled by adjusting the turbine admission valve (*kv*). Differently from the previous 5-input case, the fuel temperature (*T_fuel*) does not appear among the outputs since this variable cannot be efficiently controlled by acting on the employed inputs (Table 3).

For what the feedwater mass flow rate (*G_water*) is concerned, this input has been employed to control the steam temperature at the turbine inlet (*T_steam*). However, as indicated in the NRG

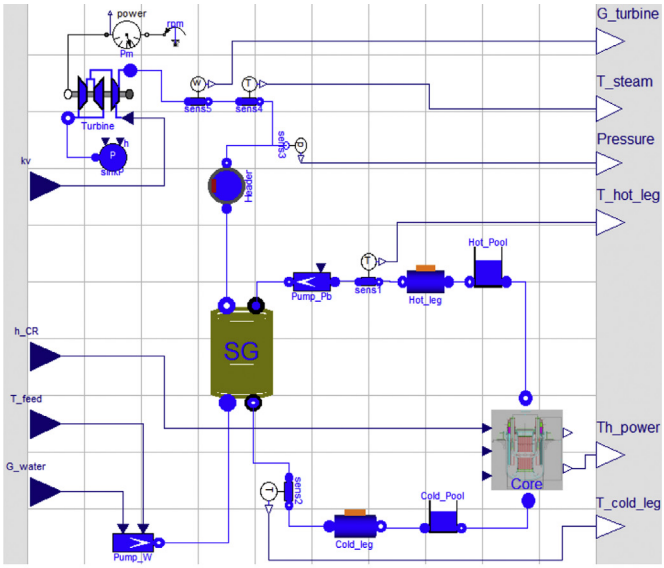

Input variables	Definition
kv	Turbine admission valve coefficient
h_CR	Control rod height
T_feed	Feedwater inlet temperature
G_water	Feedwater mass flow rate
Output variables	**Definition**
G_turbine	Turbine admitted mass flow rate
T_steam	Turbine inlet steam temperature
Pressure	SG pressure
T_hot_leg	Temperature of lead flowing out of the core
Th_power	Thermal power produced within the core
T_cold_leg	Temperature of lead flowing out of the SG

Fig. 8. Object-oriented model of the ALFRED reactor by adopting the 4-input control strategy.

Table 3
Pairing selection performed by means of the NRG method (4-input control strategy). The rows in grey represent the outputs that have been discarded for control purposes, whereas red values represent the elements that correspond to the chosen input/output pairs.

OUTPUTS	INPUTS			
	T_feed	*G_water*	*h_CR*	*kv*
T_steam	0.3966	**0.0080**	0.2098	−0.0007
Pressure	0.0000	−0.0021	0.0000	**0.9987**
G_turbine	−0.0000	0.9987	0.0000	−0.0000
T_cold_leg	**0.1623**	−0.0027	0.0586	0.0012
Th_power	0.3529	−0.0002	**0.6407**	0.0000
T_hot_leg	0.0881	−0.0018	0.0908	0.0008

outcomes (Table 3), the level of interaction does not allow to create an efficient feedback control loop. For this reason, an additional feedforward control action has been performed, as it will be described in sub-section 6.2.

6. Feedforward-feedback control scheme

As following step of the control system design procedure, the ALFRED decentralized control scheme has been implemented in SIMULINK® environment (MATLAB® and SIMULINK® software, 2005), as shown in Fig. 9. The regulator design has been developed based on a feedforward-feedback scheme incorporating four closed feedback loops with implemented PI controllers whose inputs are the following: the position of CRs, the turbine admission valve coefficient, the feedwater temperature for both the control schemes, and additionally the lead mass flow rate for the 5-input control scheme (Fig. 9a) and the feedwater mass flow rate for the 4-input control scheme (Fig. 9b). Starting from the results of the NRG analysis, it has been decided to incorporate in the control scheme a feedforward control action on the feedwater mass flow rate. As a major result, this scheme would assure an efficient control of the electric power at the alternator and an easier temperature control at the steam generator outlet. In particular, for the 4-input scheme, this configuration turns out to be necessary since the NRG outcomes show that a feedback control loop between the feedwater mass flow rate and the steam temperature would not be particularly effective (Table 3).

6.1. Proportional-integral feedback control action

The implemented control system is made up of a battery of feedback loops in which PI[1] controllers are adopted. The corresponding control law is given by:

$$u(t) = K_P e(t) + K_i \int_0^t e(t)\mathrm{d}t \tag{7}$$

where $u(t)$ represents the value assumed by the control variable, $e(t)$ is the difference between the set-point signal and the instantaneous value of the output variable, K_p is the gain of the proportional controller, and K_i is the integrator gain. The controller parameters, K_p and K_i, have been tuned on the linearized system, and then the proposed control system performance has been tested adopting the object-oriented model presented in Section 3. These PI regulators are used when the integral action is essential to provide good static performance, but, at the same time, the presence of a zero in the corresponding transfer function is necessary to grant a wider bandwidth compared with the one obtainable by adopting a simple integral action. Moreover, it is important that the error between the set-point signal (e.g., the power requested) and the instantaneous value of the output (e.g., the power produced within the core) vanishes at the end of the transients (Åström and Hägglund, 1995). The PI controllers gains have been tuned in order to achieve a large phase margin so as to get good performance even in operational conditions quite different from the nominal one. In addition, because of the tight connection between the phase margin and the damping, the choice of adopting a considerable phase margin permits to avoid excessive overshooting during transients which may jeopardize the integrity of some components (e.g., the pressure in the SGs). Finally, considering the previous constraints, the cut-off frequencies have been optimized so as to reduce the transient time of the controlled transients. The characteristic times of the PIs have been considered less relevant in the tuning process since the stability, the robustness, and the absence of oscillations in the controlled transient have been favoured in the control design.

As far as the control of inlet lead temperature (*T_cold_leg*) and steam temperature (*T_steam*) is concerned, an anti-windup has been necessarily inserted in the respective control loop to limit overshooting[2] (Fig. 9a–b). The gains and parameters of the adopted controllers are listed in Tables 4 and 5.

Among the several figures of merit of the SISO controllers, the settling time and the maximum delay have been selected for the different control loops (Table 6). The former is defined as “the time required for the response curve to reach and stay within a 2% of the final value” (Ogata, 2009). This value constitutes an indication of the time required to consider a controlled transient finished. In particular, the 5-input scheme allows obtaining more rapid controlled transients even with comparable robustness features (i.e., phase margin) respect to 4-input scheme. Indeed, as far as the lead temperature at the SG outlet and steam temperature are concerned, in the 5-input scheme, the system reaches a new stationary condition 200 s earlier than in the 4-input scheme. In this way, for what the primary circuit and turbine safety issues are regarded, it is possible to ensure that the working condition diverges for a shorter time from the nominal set-point.

The second figure of merit is represented by the maximum admissible time delay for the considered control loop beyond which it loses its asymptotic stability properties. Besides taking into account the uncertainties in the estimation of the time lag between the SG outlet and the core inlet, this aspect has to be considered for the feedback loop dedicated to the lead temperature control in case the lead mass flow rate (*G_Pb*) is employed as a system input. The time delays due to the transport phenomena in the hot and cold collectors depend on the coolant mass flow rate in the primary circuit. Therefore, in the proposed 5-input control strategy, if the lead mass flow rate is reduced, the lead speed in the collectors drops and the time delay between core and SG increases. Performing the same operational transient in nominal conditions and in partial load conditions (in which the lead mass flow rate is reduced), the system stability turns out to be quite different. Indeed, in partial load conditions, the allowable delay tends to decrease, thus making the system less robust

[1] A derivative (D) controller turns out to be useful when the reference signal varies with a high frequency and it is necessary that the system quickly follows it. In a nuclear power plant, the reference signals always have characteristic time constants of the order of seconds, and thus the proportional (P) controller and the integrator (I) are sufficient.

[2] Such a situation occurs when large changes in set-points take place and the integral term accumulates a significant error, which causes overshooting to be kept increasing.

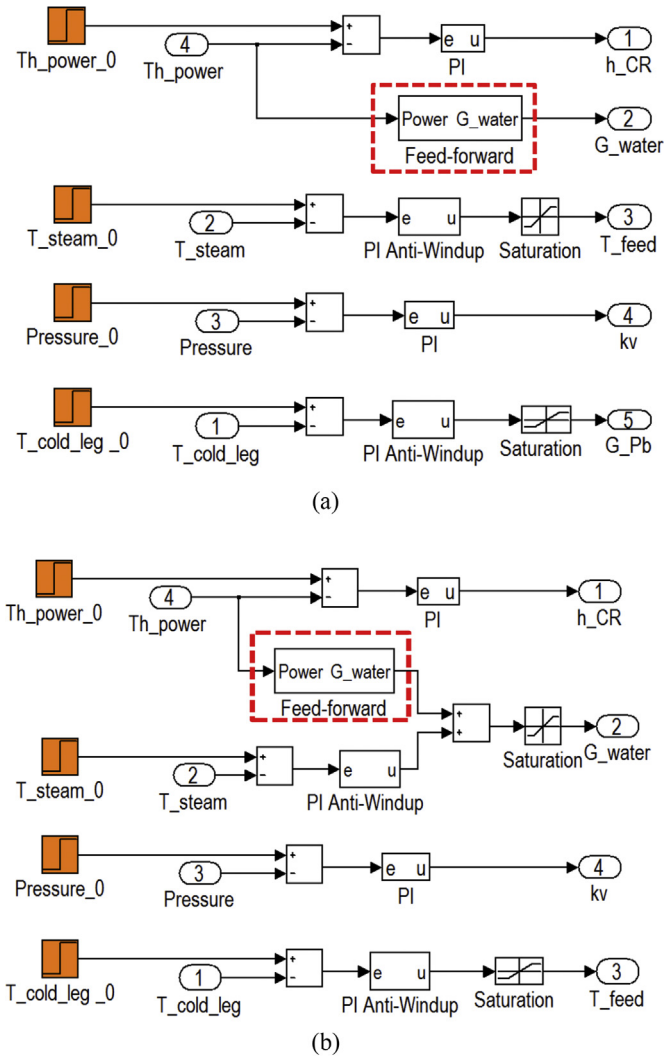

Fig. 9. Feedback loops of the developed control strategy, (a) 5-input scheme, (b) 4-input scheme.

against any uncertainties related to the timing involved in the controlled process.

6.2. Feedforward control action

Once having tuned the PI controllers gains, the feedforward scheme has been implemented. This control action consists of an algebraic law that defines the water mass flow rate as a function of the thermal power produced within the core, similar to the approach adopted in Cammi et al. (2006), ensuring a more limited use by the PI controller:

$$\Delta h^{\mathrm{ref}} \cdot G\_water = \left(T\_hot\_leg - T\_cold\_leg^{\mathrm{ref}}\right) \cdot c_p \cdot G\_Pb \tag{8}$$

where Δh^{ref} is the reference value for the enthalpy drop along the SG, $T\_cold\_leg^{\mathrm{ref}}$ is the reference value for the lead temperature in the cold leg, and c_p is the specific heat of the coolant. As shown in Table 2, as far as the 4-input scheme is concerned, the control of the steam temperature (*T_steam*) is rather ineffective because the most efficient input (i.e., *T_feed*) has to be employed for the control of the lead temperature in the cold leg (*T_cold_leg*), and the last available input (i.e., *G_water*) shows a very low pairing coefficient. For this reason, the steam temperature cannot be properly controlled, and

Table 4
Parameters of the PI controllers (4-input scheme).

Control loop		Controller gain		Controller performance	
Controlled variable	Control variable	K_p	K_i	Phase margin [°]	Cut-off frequency [rad s^{-1}]
T_cold_leg [°C]	T_feed [°C]	3	$1 \cdot 10^{-2}$	122	$8.1 \cdot 10^{-3}$
T_steam [°C]	G_water [kg s^{-1}]	$-2 \cdot 10^{-1}$	$-2 \cdot 10^{-3}$	90	$2.3 \cdot 10^{-3}$
Th_power [W]	h_CR [cm]	$-2 \cdot 10^{-11}$	$-4 \cdot 10^{-11}$	109	$3.2 \cdot 10^{-3}$
Pressure [Pa]	kv [−]	$-3 \cdot 10^{-7}$	$-1 \cdot 10^{-8}$	104	$5.4 \cdot 10^{-1}$

Table 5
Parameters of the PI controllers (5-input scheme). In the table the parameters of the four feedback control loops are reported, since the feedwater mass flow rate (G_water) performs a feedforward control action.

Control loop		Controller gain		Controller performance	
Controlled variable	Control variable	K_p	K_i	Phase margin [°]	Cut-off frequency [rad s^{-1}]
T_cold_leg [°C]	G_Pb [kg s^{-1}]	250	20	116	$2 \cdot 10^{-2}$
T_steam [°C]	T_feed [°C]	1	$6 \cdot 10^{-4}$	142	$1.6 \cdot 10^{-3}$
Th_power [W]	h_CR [cm]	$-2 \cdot 10^{-11}$	$-4 \cdot 10^{-11}$	109	$3.2 \cdot 10^{-3}$
Pressure [Pa]	kv [−]	$-3 \cdot 10^{-7}$	$-1 \cdot 10^{-8}$	104	$5.4 \cdot 10^{-1}$

Table 6
PI figures of merit.

Control loop		Control scheme	Figures of merit	
Controlled variable	Control variable		Settling time [s]	Maximum delay [s]
T_cold_leg [°C]	T_feed [°C]	4-inputs	465	265
T_cold_leg [°C]	G_Pb [kg s^{-1}]	5-inputs	200	100
T_steam [°C]	G_water [kg s^{-1}]	4-inputs	2225	680
T_steam [°C]	T_feed [°C]	5-inputs	2025	1550
Th_power [W]	h_CR [cm]	Both	1315	595
Pressure [Pa]	kv [−]	Both	10	5

one of the system inputs results to be uncoupled. In this perspective, it has been decided to use the feedwater mass flow rate to control the electric power available at the alternator (P_m) by adopting a suitable feedforward scheme for the 5-inputs as well. The value assumed by this variable can be simply derived from the following relation:

$$P\_m = \eta_0 \cdot \eta_{t,i} \cdot G\_water \cdot \Delta h_{ad} \tag{9}$$

where η_0 is the electric efficiency of the alternator, $\eta_{t,i}$ is the turbine iso-entropic efficiency, and Δh_{ad} is the enthalpy difference between turbine inlet and outlet. Because of the relevance of the electrical power in a nuclear plant, it has been disposed that the ratio between the thermal power produced within the core and the electrical power at the alternator remains constant, at any different working condition. In this way, since the feedwater mass flow rate is linearly updated according to the value of the exchanged thermal power, the electrical power at the alternator can be adjusted by regulating the thermal power produced in the core through the handling of the CRs.

7. Results of simulated operational transients

The defined feedforward-feedback control scheme has been coupled and tested on the nonlinear object-oriented model, realized by employing the Modelica language and exported in the SIMULINK® environment, as shown in Fig. 10. In order to test the performance of the two implemented schemes, two controlled operational transients have been simulated. In the former, a reduction of the reactor power from 300 MW_{th} to 250 MW_{th} has

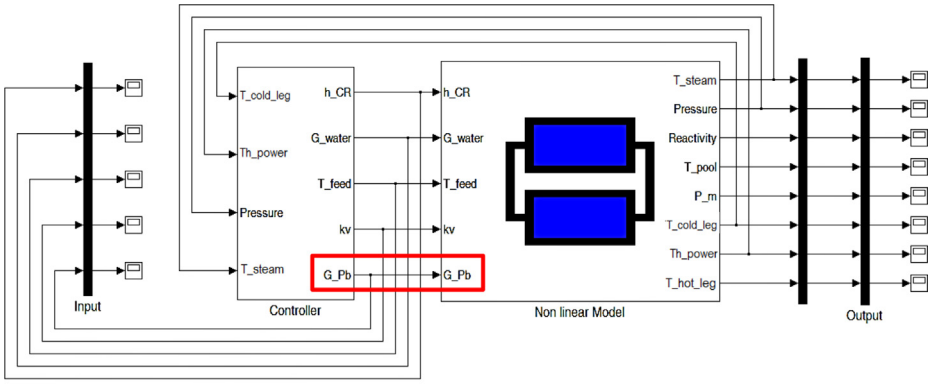

Input variables	Definition
h_CR	CR height
G_water	Feedwater mass flow rate
T_feed	Feedwater inlet temperature
kv	Turbine admission valve coefficient
G_Pb	Lead mass flow rate (5 input scheme)
Output variables	**Definition**
T_steam	Turbine inlet steam temperature
Pressure	SG pressure
Reactivity	System reactivity
T_pool	Lead temperature within the cold pool
P_m	Mechanical power produced
T_cold_leg	Temperature of lead flowing out of the SG
Th_power	Thermal power produced within the core
T_hot_leg	Temperature of lead flowing out the core

Fig. 10. Decentralized control scheme adopted for ALFRED reactor control. It is possible to notice how the difference between the two proposed strategies (use of *G_Pb*) is pointed out.

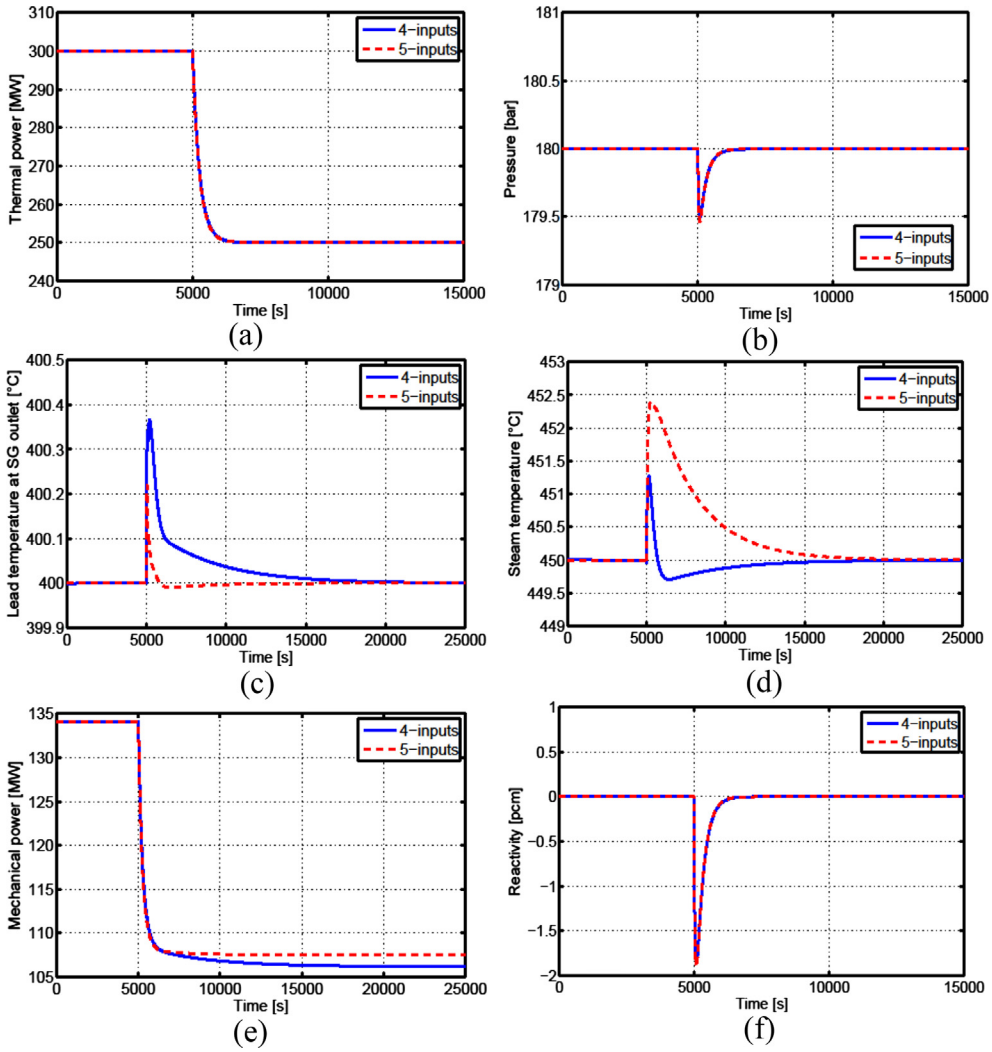

Fig. 11. Evolution of the output variables in the considered case of power level reduction: (a) reactor thermal power, (b) pressure, (c) lead temperature at the SG outlet, (d) steam temperature, (e) mechanical power, (f) reactivity.

been performed, in the latter a 5% overpower scenario has been investigated. In the following two sub-sections, for each transient, Figs. 11 to 14 show the dynamic behaviour of the controlled variables, of the control variables, as well as of other variables of interest. The red lines represent the 5-input control strategy variables, whereas the blue ones are the 4-input control strategy ones.

7.1. Power level reduction

In the first scenario, the control system effectiveness has been tested around the nominal working point, simulating an instantaneous load reduction of 50 MW_{th}. In Fig. 11a, the power transient is represented showing a settling time of 600 s for both the two schemes. Despite the differences between the two implemented control strategies, the resulting performance of the each power control loop is the same. This feature indicates the absence of coupling between this loop and the other ones, confirming the validity of the adopted decentralized control scheme. The relevant slowness of the dynamic response is partially due to the choice of reducing the control system performance in order to grant control system robustness, but it is mainly ascribed to a structural feature of the controlled physical system.

In virtue of the coupling between the primary and the secondary circuit of the plant, the SG is characterized by a very slow dynamic response as well. Nevertheless, the pressure in the SG shows a good behaviour in both control schemes (Fig. 11b). After having reached a maximum difference from the nominal value of 0.5 bar, the controlled variable settles on its nominal value of 180 bar in 1200 s (time to reach the 2% of the maximum variation). This time constant would have been reduced by simply increasing the gain parameters of PI controllers, but relevant overshooting would have occurred. Indeed, such a pressure response may constitute a concern because of the induced mechanical stresses.

As far as the power control loop is concerned, the uncoupling level is quite high and the two control schemes show a similar performance. As shown in Fig. 12a and b, respectively, no relevant discrepancies can be appreciated for the CRs insertion value and the turbine admission valve coefficient (i.e., the two control variables that regulate the reactor thermal power and the SG pressure, respectively).

On the other hand, some differences between the two control schemes can be found observing the SG outlet temperature evolution (Fig. 11c). First of all, different time constants are obtained, namely 4000 s for the 5-inputs and 12,000 s for the 4-inputs. In addition, the 4-input scheme presents a major departure from the

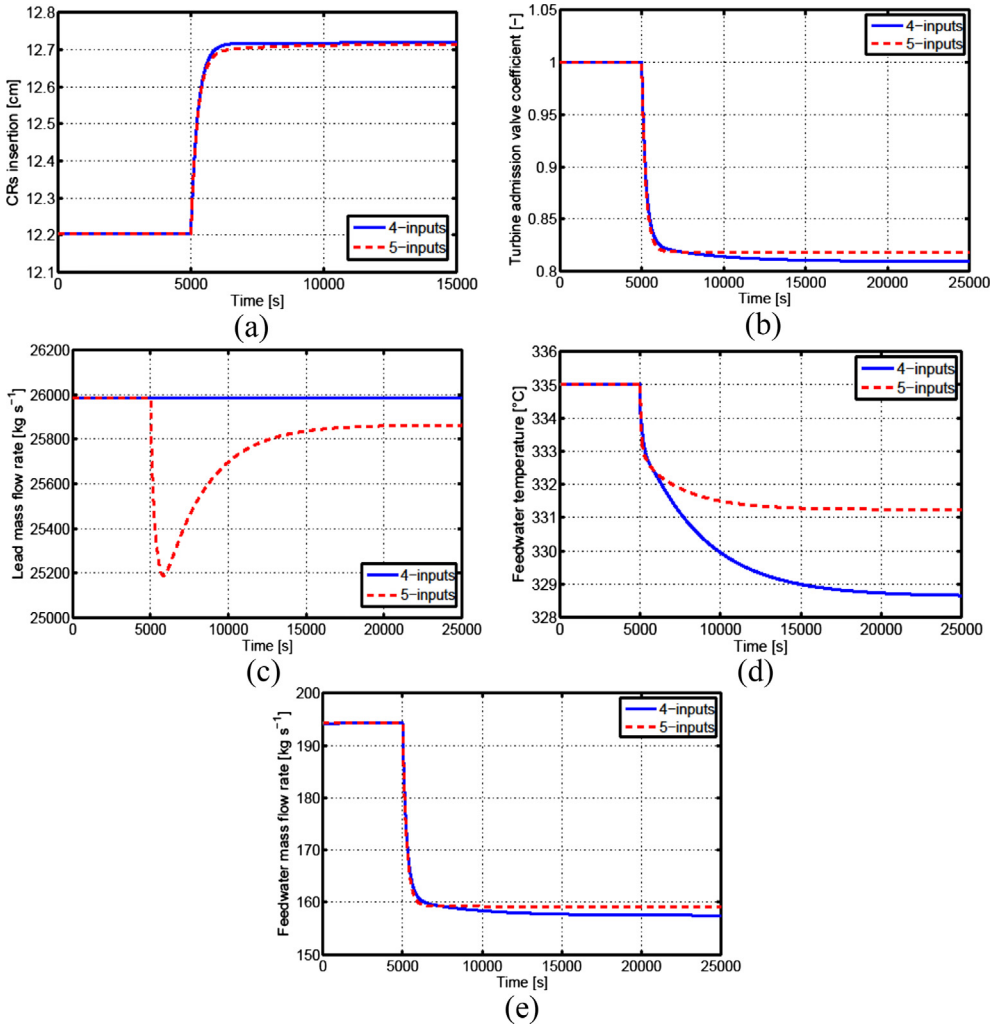

Fig. 12. Evolution of the control variables in the considered case of power level reduction: (a) CRs insertion, (b) turbine admission valve coefficient, (c) lead mass flow rate, (d) feedwater temperature, (e) feedwater mass flow rate.

nominal value in the first part of the transient. Finally, the related control variables – lead mass flow rate for the 5-inputs (Fig. 12c, red line), and the feedwater temperature for the 4-inputs (Fig. 12d, blue line) – show different evolutions, which allow pointing out the differences between the two control strategies. It is worth observing that the lead mass flow rate variation necessary to control the lead temperature is not demanding (the maximum requested variation is slightly more than the 3% of the nominal value). On the other hand, the narrow operational range of the feedwater temperature constitutes a relevant concern in the use of this variable since the steady state value is very close to the lead freezing point (327 °C). Consequently, when the lead temperature is regulated by operating on the lead mass flow rate, better control performance can be achieved in virtue of the more relevant coupling. In addition, since lead mass flow rate variations are not restricted by so severe constraints, the controlled system would present a higher level of flexibility during operational transients guaranteeing the respect of the lower limit on reactor inlet temperature.

As far as the steam temperature evolution is concerned (Fig. 11d), the best performance belongs to the 4-input models, mainly due to the reduced variations from the nominal value of 450 °C (only about 1 °C compared with more than 2 °C of the 5-input model). The settling time is quite similar between the two schemes (11,000 s for the 4-inputs, 12,000 s for the 5-inputs). As far as the control variable that most influences the steam temperature is concerned – i.e., the feedwater temperature for the 5-inputs (Fig. 12d, red line), and the feedwater mass flow rate for the 4-inputs (Fig. 12e, blue line) – there are no relevant issues.

For the sake of completeness, the responses of other output variables of interest are presented in Fig. 11e (mechanical power) and Fig. 11f (system reactivity). Since the entire steam mass flow rate is sent to the turbine and the turbine admission coefficient is devoted to the pressure control, the mechanical power evolution is characterized by the same time constant of the thermal power produced in the core. Finally, it is worth noting that the overall performed control actions limit the variation of the system reactivity (less than 2 pcm).

7.2. *Power level enhancement*

In this operational transient, the effectiveness of the proposed control schemes in an overpower scenario (enhancement by 5% of the nominal power, Fig. 13a, operating on CRs, Fig. 14a) has been evaluated. In this case, the importance of performing a control action on the lead mass flow rate circulating in the primary circuit

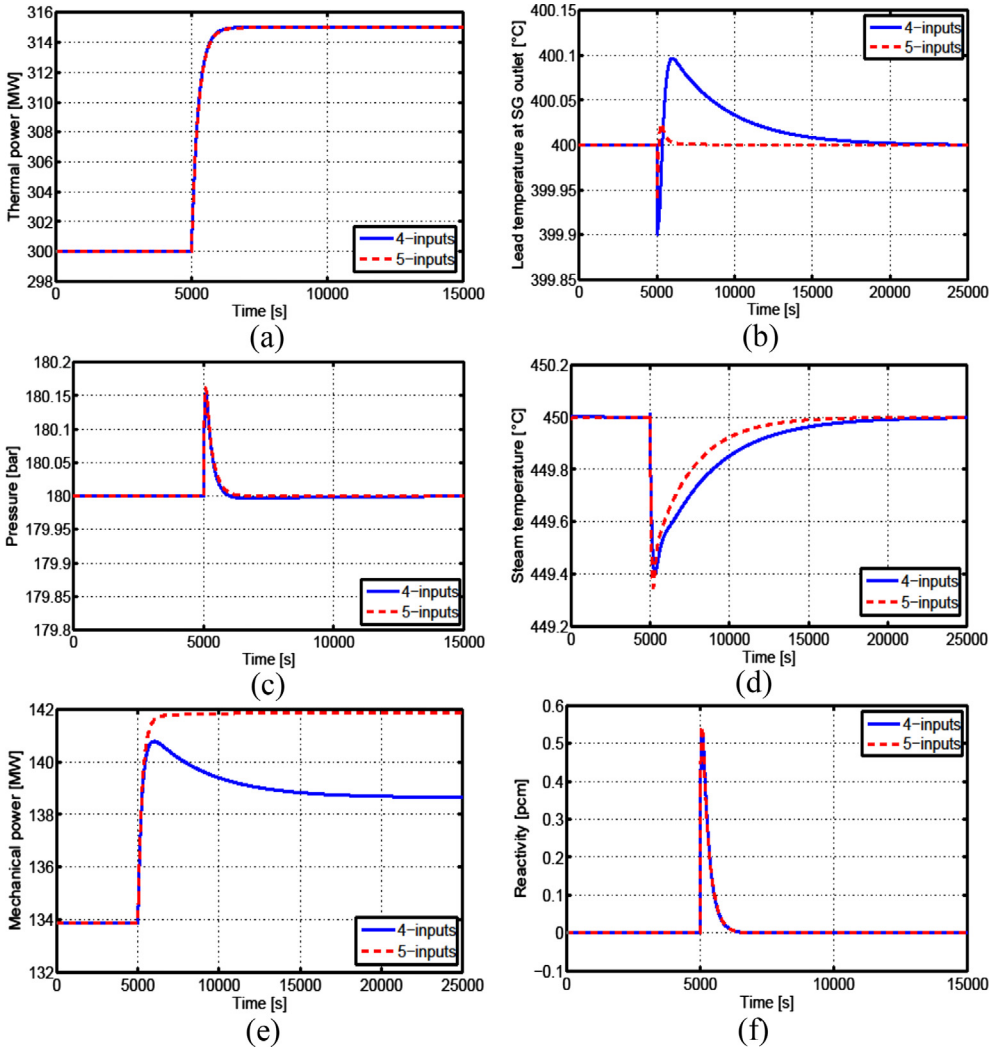

Fig. 13. Evolution of the output variables in the considered case of power level enhancement: (a) reactor thermal power, (b) lead temperature at SG outlet, (c) pressure, (d) steam temperature, (e) mechanical power, (f) reactivity.

even more clearly emerges. As it has been noticed in the outcomes of the NRG analysis (Table 2), when it is not possible to use this control variable to govern the value of the lead temperature in the cold leg, it is better to adopt the feedwater temperature. The pairing (*T_feed*, *T_cold_leg*), in addition to being less effective than the previous one (*G_Pb*, *T_cold_leg*), has not negligible consequences on the feedforward as well. In Fig. 13b, the value of the lead temperature at the SG outlet is represented and it is possible to note how the control action performed by adjusting the lead mass flow rate (Fig. 14b) allows to significantly damp the oscillations. In the 4-input scheme, following the power enhancement, the feedwater temperature (Fig. 14c, blue line) must be reduced to govern the increasing lead temperature in the cold leg (Fig. 13b, blue line), changing the secondary system boundary conditions. Then a further control action on feedwater mass flow rate and on turbine admission coefficient (Fig. 14d and e) has to be performed in order to maintain the conditions at the turbine inlet, namely the steam pressure and temperature (Fig. 13c and d).

On the other hand, by adopting the 5-input control scheme, the possibility to adjust the value of the lead mass flow rate allows reducing the oscillations of the SG lead outlet temperature (Fig. 13b, red line) and the action performed on feedwater temperature (Fig. 14c, red line). In this way, a greater water enthalpy difference in addition to a greater feedwater mass flow rate allows obtaining a better performance for what concerns the mechanical power production shown in Fig. 13e. Thanks to the proper control action performed on the interface between the primary and the secondary circuit, the lead temperature at the core inlet slightly changes and this allows increasing the power level staying close to criticality (Fig. 13f).

8. Conclusions

In this paper, a preliminary approach to the definition of a suitable control strategy for the ALFRED reactor has been presented. Lead Fast Reactors are characterized by technological issues and safety concerns which do not allow the adoption of the well-proven control strategies used in LWRs or SFRs. For this reason, after having firstly studied the system stability and dynamics of ALFRED, in the second phase of the control design, it has been decided to employ a quantitative approach based on the RGA method to find out the most effective input/output pairings. Thanks to this modelling tool currently adopted in industrial applications and recently employed in nuclear field, it has been possible to define the control strategy starting from the constitutive equations

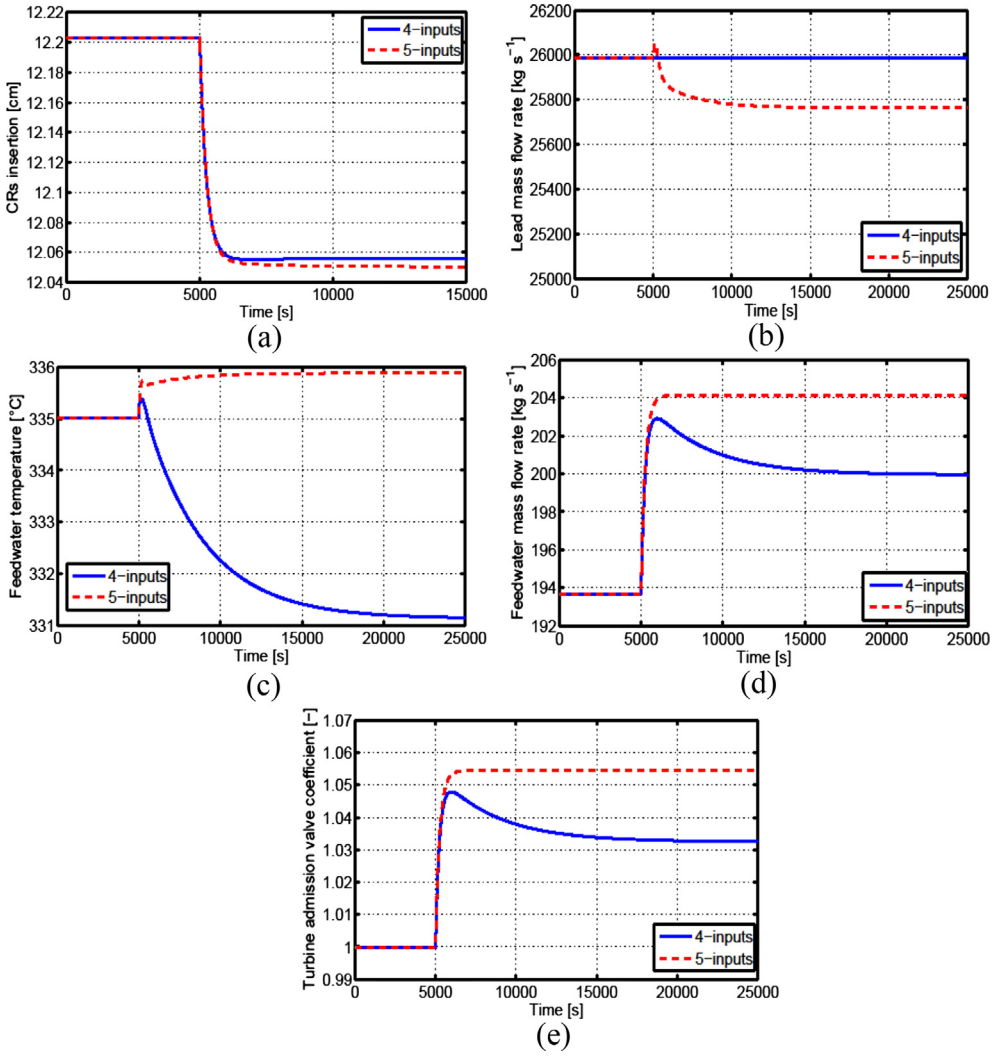

Fig. 14. Evolution of the control variables in the considered case of power level enhancement: (a) CRs insertion, (b) lead mass flow rate, (c) feedwater temperature, (d) feedwater mass flow rate, (e) turbine admission valve coefficient.

that describe the system governing dynamics. Based on the outcomes of the RGA analysis, different control strategies have been studied depending on the number of system inputs. Indeed, the possibility of adopting the lead mass flow rate in the primary loop as a control variable has been considered in a 5-input control scheme and compared with another option (4-input control scheme) in which it has been considered as a fixed parameter. The resulting control system configurations have been preliminarily ascertained by means of the object-oriented plant simulator developed by Ponciroli et al. (2014), and a classical combined feedforward-feedback scheme based on the incorporation of PI controllers has been employed. The implemented control schemes for the ALFRED reactor have been developed by adopting regulators for SISO linearized systems but, as a major achievement of this work, the performance of the developed decentralized control schemes has been evaluated by simulating typical transients. The obtained results are satisfactory, and indicate the effectiveness of both linear control systems whose suitably tuned controllers parameters grant a compromise among performance, robustness, and safety margins. Comparing the dynamic responses of control and controlled variables, the advantages of adopting the lead mass flow rate as a system input have been shown. Indeed, if it is possible to govern the lead temperature at the SG outlet without employing a secondary system input, the feedwater inlet conditions can be adopted to regulate the output variables of the balance of plant, without being conditioned by the primary circuit concerns.

In short, the results presented in this work concerning the impact of the main control variables and the development of two possible control strategies constitute a reliable starting point for the definition of the ALFRED reactor control system architecture. In the next stages, it will be necessary to confirm the preliminary indications provided by the RGA analysis. Indeed, it is important to assess that for the several control loops, the modelling techniques adopted for SISO systems are still valid at different power conditions. Finally, after the implementation of the regulators, actuators and suitable rate limiters on the performed control action will be employed in order to finalize the configuration of the control system.

Acknowledgements

The authors acknowledge the European Commission for funding the LEADER Project in the 7th Framework Programme. Acknowledgement is also due to all the colleagues of the participant organizations for their contributions in many different topics, in particular to Dr. Alessandro Alemberti and Dr. Luigi Mansani

(Ansaldo Nucleare, Italy) for their valuable support and fruitful criticism. The authors are also grateful to Mr. Alessandro Della Bona (Politecnico di Milano, Italy) for his suggestions about the control strategy definition.

References

Alemberti, A., Frogheri, M., Mansani, L., 2013. The lead fast reactor demonstrator (ALFRED) and ELFR design. In: Proceedings of the International Conference on Fast Reactors and Related Fuel Cycles: Safe Technologies and Sustainable Scenarios (FR 13), Paris, France, March 4–7, 2013.

Åström, K.J., Hägglund, T., 1995. PID Controllers: Theory, Design and Tuning. Instrument Society of America, Research Triangle Park, NC, USA.

Bernard, J.A., 1999. Light water reactor control systems. In: Webster, J.G. (Ed.), Wiley Encyclopedia of Electrical and Electronics Engineering. New York, NY, USA.

Bortot, S., Cammi, A., Lorenzi, S., Ponciroli, R., Della Bona, A., Juarez, N.B., 2013. Stability analyses for the European LFR demonstrator. Nucl. Eng. Des. 265, 1238–1245.

Bristol, E.H., 1966. On a new measure of interaction of multivariable process control. IEEE Trans. Auto. Cont. 11, 133–134.

Cammi, A., Luzzi, L., Porta, A.A., Ricotti, M.E., 2006. Modelling and control strategy of the Italian LBE-XADS. Prog. Nucl. Energy 48, 578–589.

Chang, J.-W., Yu, C.-C., 1990. The relative gain for non-square multivariable systems. Chem. Eng. Sci. 45, 1309–1323.

Damiani, L., Montecucco, M., Pini Prato, A., 2013. Conceptual design of a bayonet tube steam generator for the ALFRED lead-cooled reactor. Nucl. Eng. Des. 265, 154–163.

DYNASIM, 2006. Dymola Version 6.1. Dynasim AB, Lund, Sweden. Homepage: http://www.dynasim.se (accessed 16.12.13.).

Elmqvist, H., Cellier, F.E., Otter, M., 1993. Object-oriented modeling of Hybrid systems. In: Proceedings of the European Simulation Symposium (ESS'93), Delft, Netherlands, October 25–28, 1993.

Fritzson, P., 2004. Principles of Object-oriented Modeling and Simulation with Modelica 2.1. Wiley-IEEE Press.

GIF, 2002. A Technology Roadmap for Generation IV Nuclear Energy Systems. Technical Report GIF-002-00.

Grasso, G., Petrovich, C., Mikityuk, K., Mattioli, D., Manni, F., Gugiu, D., 2013. Demonstrating the effectiveness of the European LFR concept: the ALFRED core design. In: Proceedings of the International Conference on Fast Reactors and Related Fuel Cycles: Safe Technologies and Sustainable Scenarios (FR 13), Paris, France, March 4–7, 2013.

Guerrieri, C., Cammi, A., Luzzi, L., 2014. A preliminary approach to the MSFR control issues. Ann. Nucl. Energy 64, 472–484.

Laub, A.J., Heath, M.T., Paige, C.C., Ward, R.C., 1987. Computation of system balancing transformations and other applications of simultaneous diagonalization algorithms. IEEE Trans. Auto. Cont. AC-32, 115–122 (accessed 13.12.13.). http://www.leader-fp7.eu/.

Lewins, J., 1978. Nuclear Reactor Kinetics and Control. Pergamon Press Ltd., Oxford, UK.

MATLAB® and SIMULINK® Software, 2005. The MathWorks, Inc.

Moore, B.C., 1981. Principal component analysis in linear systems: controllability, observability, and model reduction. IEEE Trans. Auto. Cont. AC-26 (1), 17–32.

Ogata, K., 2009. Modern Control Engineering. Prentice Hall.

Papadourakis, A., Doherty, M.F., Douglas, J.M., 1987. Relative gain array for units in plants with recycle. Ind. Eng. Chem. Res. 26 (6), 1259–1262.

Ponciroli, R., Bigoni, A., Cammi, A., Lorenzi, S., Luzzi, L., 2014. Object-oriented modelling and simulation for the ALFRED dynamics. Prog. Nucl. Energy 71, 15–29.

Skogestad, S., Postlethwaite, I., 2005. Multivariable Feedback Control: Analysis and Design. John Wiley and Sons, New York, USA.

Tucek, K., Carlsson, J., Wider, H., 2006. Comparison of sodium and lead-cooled fast reactors regarding reactor physics aspects, severe safety and economical issues. Nucl. Eng. Des. 236, 1589–1598.

Van Dooren, P., 2000. Gramian based model reduction of large-scale dynamical systems. In: Watson, G.A., Griffiths, D.F. (Eds.), Numerical Analysis 1999, Chapman & Hall/CRC Research Notes in Mathematics Series, London, pp. 231–247.